ASM Sc. J., 17, 2022

https://doi.org/10.32802/asmscj.2022.1351

Effect Of Carbon Content on The Impact Energy of Ductile Austenitic Cast Iron

K.M. Khaled*, R.S. Hegazy and M. Mohamed

National Institute of Standards (NIS), Egypt

In the present investigation, the effect of varying the carbon content on the impact energy of ductile cast iron was studied. Three groups of ductile austenitic cast iron (A), (B) and (C) were prepared for Charpy impact tests. The carbon equivalent percent (% CE) for group (A) ranged from 3.51 to 5.04 and the variable element was carbon, whereas the % CE for group (B) is ranged from 3.86 to 4.64 and the variable element was silicon, and the % CE for group (C) is ranged from 3.79 to 4.80 and the variable element was nickel. Results show that there is an inverse proportional relation between the absorbed impact energy and the % CE if silicon or nickel are used as variable elements, while this relation remains constant when using carbon as variable element to control the value of % CE.

Keywords: Ductile austenitic cast iron; absorbed energy; impact test; certified reference material

I. INTRODUCTION

Ductile austenitic cast iron is a chain of cast irons that contain nickel from 18 to 36 percent of weight, which has been treated with magnesium to create nodular graphite rather than standard angular graphite (AFS, 2010; ASM International, 1990; ASM International, 2004). Characterisation of the mechanical properties of this material consider important to widen the fields of application. Ductile austenitic cast iron contains enough nickel to make the matrix structure of the austenitic iron which is similar to the matrix structure of the austenitic stainless steel. This iron has a tensile strength of 370 MPa to 560 MPa, and 4 to 40 elongation percent, and 1110 MPa to 1710 MPa Brinell hardness number (ASM International, 2004). Such ductile high-nickel alloyed cast iron is made to produce the desired properties in many varied compositions, although traditional foundry methods are used to manufacture Ni-resistant ductile iron castings with special precautions. Treatment practices, temperature release and gating practices should be substantially improved from the traditional ductile cast iron practices. Consequently, proposed casting designs should be checked by designers and producers of Ni-resist ductile austenitic cast iron whether both minimum cost and maximum product quality are to be achieved (AFS, 2010; ASM International, 1990; ASM International, 2004). Many data on mechanical properties and microstructure of ductile cast iron have been published (AFS, 2010; ASM International, 1990; ASM International, 2004; Angus, HT, 1978; Karsay, SI, 1987; Bayati, H & Elliott, R, 1995). The study and development of austempered ductile cast iron was the most recent research (Bai, J *et. al.,* 2022; Zhou, W *et. al.,* 2021; Fatahalla, N *et al.,* 1998). Few scientists are interested in investigating the production techniques, microstructure, and the mechanical properties of ductile austenitic cast iron focusing on a constant carbon equivalent of 4.3 (% CE) closes to the eutectic composition (Fatahalla, N *et. al.,* 1998; Zeng, DW *et. al.,* 2002; Hua, Q *et. al.,* 2005; Karaman, I *et. al.,* 2001; Alzafin, YA *et. al.,* 2009; Ahmed, KM *et. al.,* 2016; Moumeni, E, 2013; Fatahalla, N *et al.,* 2009). Therefore, there is a lack of identifying the mechanical properties of ductileaustenitic cast iron produced from % CE close to the eutectic composition. This investigation focused on use C, Si and Ni as alloying elements to vary the carbon equivalent and study its effect on the absorbed energy of ductile austenitic cast iron. Another objective of the current investigation is to extend the scope of applications of ductile austenitic cast iron alloys to be used as certified reference material (standard block) to verify the performance of pendulum impact testing machines.

*Corresponding author's e-mail: khaled_fmmd_nis@yahoo.com

II. MATERIALS AND METHODS

A. Sampling and Mounting

The Y-block castings for all heats were machined to cut off the head of Y-block and the other part was divided into equal transverse bars of dimensions (12 × 12.5 × 179) mm. Specimens from the top of the middle bar of cubic shape of dimension 10 mm were cut off and mounted in Bakelite mould 25 mm diameter.

The rough grinding was performed until the surfaces of the specimens were flat and all scratches due to cut-off disappeared. Progressive grinding, using light hand pressure, with a series of silicon carbide (SiC) papers containing finer abrasive grits, on a motor-driven wheel was conducted. The grinding sequence was performed with grain sizes 160, 220, 320, 400, 600, 800 and 1000 mesh. Water was used through all grinding stages from 160 up to 1000. Grinding wheel speeds were 150 and 300 rpm.

After grinding process, the specimens were cleaned with water and dried with hot air. Then, it was rough polished on a rotating wheel covered with napless cloth and charged with 8, 6, and 1μm diamond paste abrasive. The polishing cloth (napless) is damped with diamond lubricant blue during rough polishing process. After rough polishing was finished, fine polishing was performed using a suspension of 0.03 μm Al_2O_3 on a wet short nap cloth. At completion of polishing operation, specimens were rinsed with alcohol and dried in a stream of warm air.

Microstructure examination and photomicrography of the polished specimens were carried out after etching. Chemical etching was performed by swabbing the specimens for about 12 seconds with nital (5 volume % concentrated nitric acid and 95 mass % alcohol) (Karsay, SI 1987). After etching, specimens were rinsed in running water, alcohol and then dried in a stream of warm air.

Reichert MeF2 universal optical microscope was used in all metallographic examinations carried out through the present study. Optical camera of high resolution was fixed and adapted to the optical microscope to photo all polished specimens with magnification up to 1500×, then photos obtained by digital camera were connected to computer and with special program converted its format to JPEG format with varied magnifications. Special optical scale of 0.1 mm length was used to calibrate the magnifications of optical microscope and to calculate the actual magnification of all microstructure photos in this study. Microstructures were examined, for all tested specimens, in both as- polished and as-etched conditions.

The number of nodules per unit area was determined by counting the number of nodules on the photographs at a magnification of about 200× and then calculating the number of nodules per square millimetre. To determine the nodule size, all nodules of different sizes were measured manually at suitable magnification by using computer program, and the average was taken.

B. Experimental Work

The % CE values are calculated according to the following equation:

$$\% CE = C\ \% + 0.33\times Si\ \% + 0.047\times Ni\ \% - 0.0055\times Ni\ \% \times Si\ \% \quad (1)$$

To assess the effect of iron composition (% CE), on the energy absorbed of ductile austenitic cast iron, three groups (A, B and C), five impact Charpy specimens were machined for impact test for each heat group. Impact tests were carried out according to ISO 148-1:2016 Metallic materials – Charpy pendulum impact test - Part 1: Test method (ISO 148-1:2016) by Roell/Amsler Charpy pendulum impact machine shown in Figure 1. The standard test piece shall be 55 mm long and of square section, with 10 mm sides. In the centre of the length, there shall be a V-notch. Table 1 shows the standard grades of ductile austenitic cast iron mentioned in ASTM A439 [ASTM A439 / A439M – 18]. Table 2 shows the chemical composition of the 3 groups of ductile austenitic cast iron produced in the current study.

Figure 1. Charpy impact test machine

Table 1. Common energy absorbed values for ductile austenitic cast irons according to ASTM A439 / A439M – 18

Type	% CE	Energy absorbed (J)
D2	4.44	14-27
D2B	4.44	12
D2C	4.37	21-33
D3	4.33	8
D3A	4.92	16
D4	4.33	-
D5	4.31	20
D5B	4.31	7
D5S	3.17	12-19
Ductile austenitic cast iron (18)	4.21	16

Table 2. The chemical composition of the produced 3 groups of ductile austenitic cast iron

Group symbol	Heat number	Composition				
		Ni	C	Si	Mn	Mg
A	A1	19.77	2.11	2.12	1.40	0.043
	A2	19.44	2.31	2.07	1.40	0.041
	A3	19.41	2.53	2.11	1.40	0.045
	A4	19.70	2.71	2.08	1.40	0.050
	A5	19.54	2.95	2.12	1.40	0.045
	A6	19.41	3.16	2.14	1.40	0.053

	A7	19.52	3.29	2.08	1.40	0.048
	A8	20.02	3.42	2.16	1.40	0.059
B	B1	21.54	2.50	1.63	1.34	0.047
	B2	21.59	2.53	2.17	1.33	0.040
	B3	21.90	2.52	2.76	1.32	0.042
	B4	21.67	2.56	3.32	1.33	0.049
	B5	21.86	2.54	3.89	1.34	0.051
	B6	21.87	2.51	4.41	1.34	0.049
	B7	21.65	2.53	4.92	1.33	0.038
	B8	21.58	2.50	5.31	1.33	0.036
C	C1	4.99	2.90	1.86	1.77	0.045
	C2	9.09	2.85	1.82	1.72	0.069
	C3	13.50	2.79	1.84	1.48	0.061
	C4	16.10	2.80	1.85	1.56	0.065
	C5	19.80	2.83	1.75	1.71	0.051
	C6	23.90	2.78	1.79	1.60	0.063
	C7	30.40	2.77	1.85	1.59	0.067
	C8	34.70	2.91	1.83	1.39	0.062

III. RESULTS AND DISCUSSION

There were three groups of ductile austenitic cast iron and each group contains eight different % CE heats. The key parameter was (i) carbon percent (group A), (ii) silicon percent (group B) and (iii) nickel percent (group C). Table 3 lists the close values of nominal and real % CE of group A, B and C, respectively. Figure 2 to Figure 4 show the microstructures of the three groups and clearly show the imbedded graphite nodules. Furthermore, Figure 2 to Figure 4 show the low effect of % CE variation on the nodule-count presented in ductile austenitic cast iron. Table 4 shows the effect of % CE on nodule-count, nodule-size and nodularity of all ingots.

Table 3. Nominal and actual carbon equivalent % CE for groups A, B, and C

Description	**Group (A)**		**Group (B)**		**Group (C)**	
	Nominal % CE	Actual % CE	Nominal % CE	Actual % CE	Nominal % CE	Actual % CE
1	3.50	3.51	3.55	3.86	3.52	3.70
2	3.70	3.69	3.73	4.00	3.72	3.79
3	3.90	3.91	3.92	4.16	3.92	3.90
4	4.10	4.10	4.11	4.28	4.12	4.00

5	4.30	4.34	4.31	4.38	4.32	4.15
6	4.50	4.55	4.52	4.46	4.52	4.26
7	4.70	4.67	4.71	4.59	4.72	4.49
8	4.90	5.04	4.92	4.64	4.92	4.80

Table 5 summarises the influence of % CE ranging from 3.51 to 5.04 on the absorbed energy of all heats group A: varied carbon percent (C %) from 2.11 to 3.42. Figure 5 shows the influence of % CE on the energy absorbed for the ductile austenitic cast iron used in the current study for group A. It can be seen that there is almost no variation in absorbed energy values with the variation of % CE. This may stem from the approximately fully austenitic matrix of all heats and due to 100 % nodularity of all heats of this group from % CE 3.51 to 5.04. This is believed to refer to the fully austenitic matrix observed in all microstructures. On the other hand, the absorbed energy values are ranging from 19 J to 22 J.

Table 6 summarises the effect of % CE from 3.86 to 4.64 on the energy absorbed of all heats for group B: varied silicon percent (Si %) from 2.50 to 5.31. It is clear from Table 4 and Figure 6 that the absorbed energy values fall between 12 J and 27 J. It is also observed that the absorbed energy decreases with increasing the % CE to reach the lowest value at 4.64 % CE, this decrease may be due to the increase of Si % and nonhomogeneous distribution of nodules and fully austenitic matrix, the highest value of absorbed energy is at 4.16 % CE which may stem from the optimum amount of this heat Si %.

Table 7 summarises the effect of % CE from 3.79 to 4.80 of all heats for group C: varied nickel percent (Ni %) from 9.09 to 34.70. It can be seen that the absorbed energy values are falls between 7 J and 27 J. Figure 7 shows that the absorbed energy slightly increased to reach a stable value around 25 J for the % CE ranging from 3.90 to 4.15, then decrease dramatically to reach another stable value around 9 J for the % CE ranging from 4.26 to 4.80. This implies may be due to the jump expansion in the nodule count (count of nodule/ area in mm^2) from 200, for the heat C2-C5, to 250 for the heats C6-C8.

The values of all groups agree with the same range of standard grades of ductile austenitic cast iron mentioned in ASTM A439 (ASTM A439 / A439M – 18) shown in Table 1.

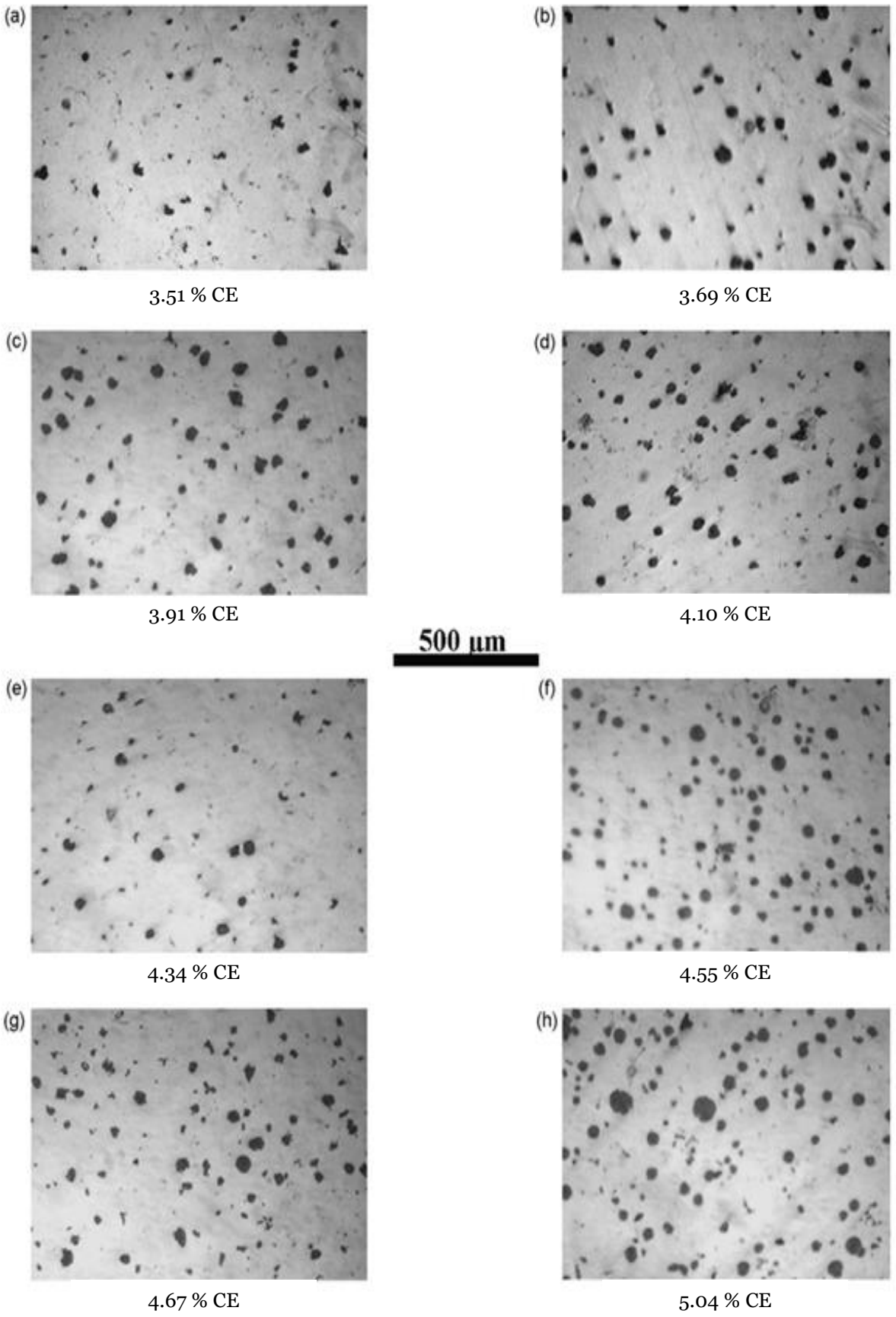

Figure 2. Microstructure of group A, varied C% from 2.11 to 3.42 to change the % CE from 3.51 to 5.04

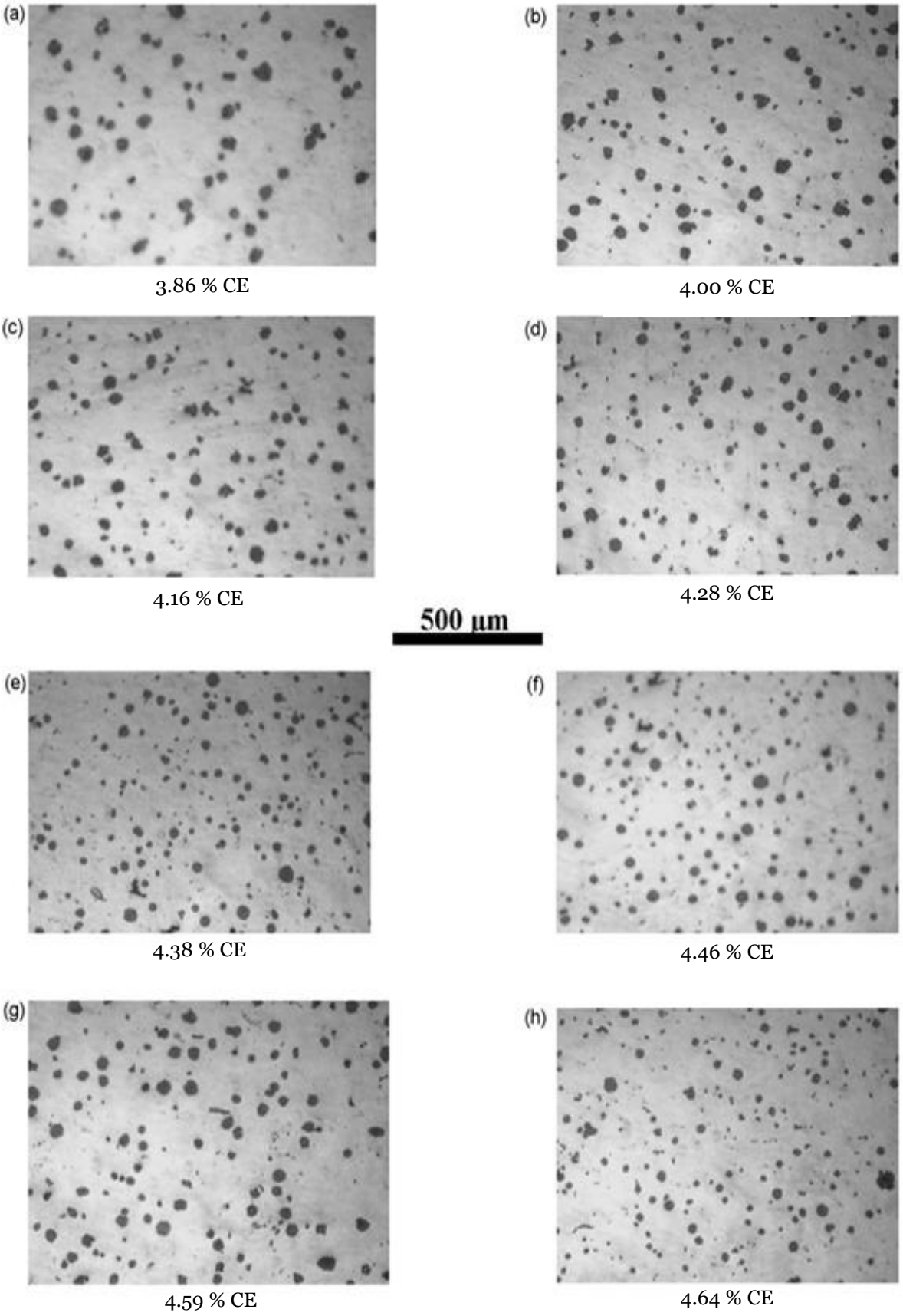

Figure 3. Microstructure of group B, varied Si % from 1.63 to 5.31 to change the % CE from 3.86 to 4.64

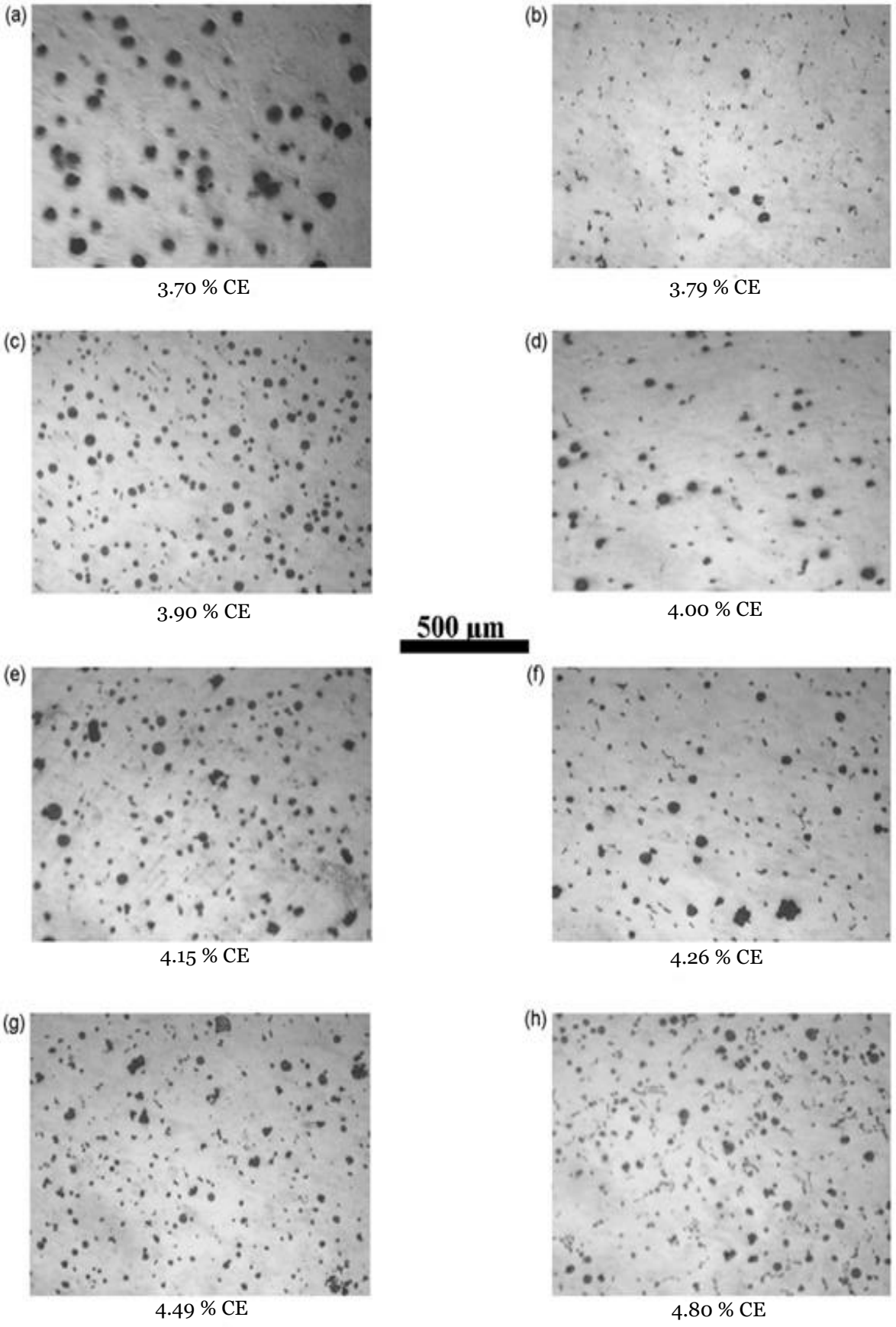

Figure 4. Microstructure of group C, varied Ni % from 4.99 to 34.70 to change the % CE from 3.70 to 4.80

Table 4. Effect of % CE on nodule-count, nodule-size and nodularity of all ingots

Group symbol	Heat no.	% CE	Nodule count nodule/mm²	Nodule size µm	Nodularity %
A	A1	3.51	80	15	80
	A2	3.69	125	28	100
	A3	3.91	125	25	100
	A4	4.10	125	25	100
	A5	4.34	70	20	100
	A6	4.55	220	25	100
	A7	4.67	220	25	100
	A8	5.04	220	25	100
B	B1	3.86	130	28	100
	B2	4.00	160	25	100
	B3	4.16	200	25	100
	B4	4.28	200	25	100
	B5	4.38	225	22	100
	B6	4.46	225	22	100
	B7	4.59	225	22	100
	B8	4.64	250	20	100
C	C1	3.70	125	28	100
	C2	3.79	200	10	100
	C3	3.90	250	15	100
	C4	4.00	180	15	100
	C5	4.15	200	15	100
	C6	4.26	250	15	100
	C7	4.49	250	15	100
	C8	4.80	250	15	100

Table 5. The effect of changing the % CE from 3.51 to 5.04 on the absorbed energy of all heats for group A, varied carbon percent (C %) from 2.11 to 3.42

Composition	C%	% CE	Average energy absorbed (J)	Standard deviation (J)
A1	2.11	3.51	20.067	1.677
A2	2.31	3.69	20.133	2.491
A3	2.53	3.91	22.167	0.764
A4	2.71	4.10	19.433	1.290
A5	2.95	4.34	21.900	2.261
A6	3.16	4.55	19.200	0.721
A7	3.29	4.67	21.667	1.528
A8	3.42	5.04	19.800	2.117

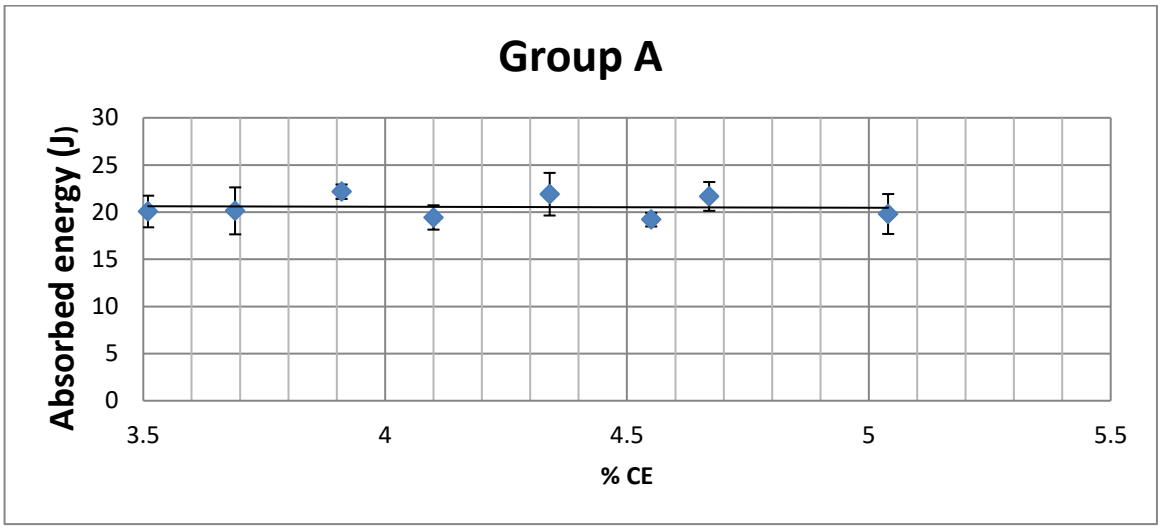

Figure 5. The effect of changing the % CE from 3.51 to 5.04 on the absorbed energy of all heats for group A, varied carbon percent (C %) from 2.11 to 3.42

Table 6. The effect of changing the % CE from 3.86 to 4.64 on absorbed energy of all heats for group B, varied silicon percent (Si %) from 1.63 to 5.31

Composition	Si %	% CE	Average Charpy Impact (J)	Standard deviation (J)
B1	1.63	3.86	26.125	1.652
B2	2.17	4.00	26.100	1.709
B3	2.76	4.16	27.000	2.000
B4	3.32	4.28	24.943	2.561
B5	3.89	4.38	22.043	2.909
B6	4.41	4.46	21.333	2.082
B7	4.92	4.59	18.650	3.041
B8	5.31	4.64	12.700	2.211

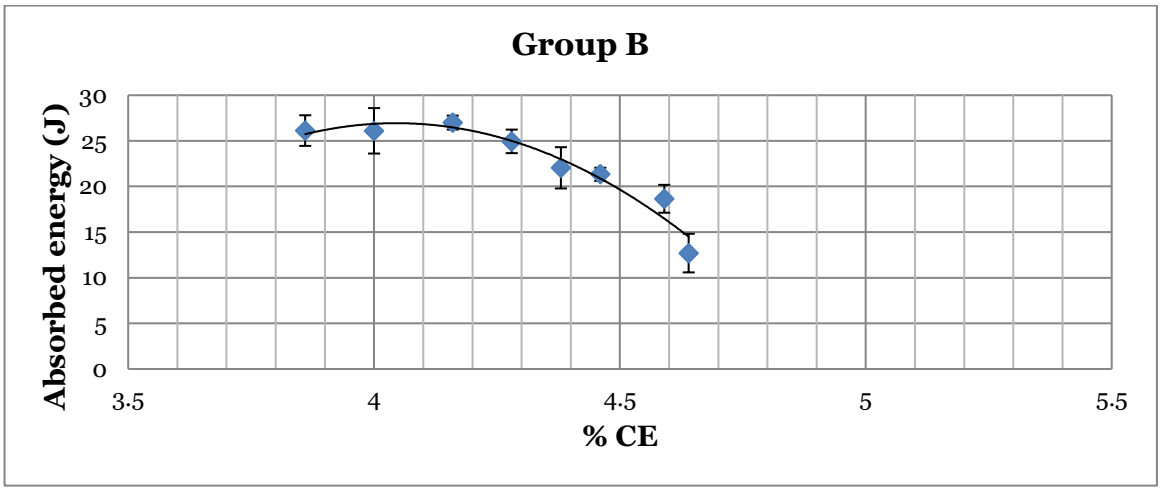

Figure 6. The effect of changing the % CE from 3.86 to 4.64 on absorbed energy of all heats for group B, varied silicon percent (Si %) from 1.63 to 5.31

Table 7. The effect of changing the % CE from 3.70 to 4.80 on absorbed energy of all heats for group C, varied nickel percent (Ni %) from 4.99 to 34.70

Composition	Ni %	% CE	Average Charpy Impact (J)	Standard deviation (J)
C1	4.99	3.70	-	-
C2	9.09	3.79	17.333	0.289
C3	13.50	3.90	26.700	0.173
C4	16.10	4.00	27.500	0.866
C5	19.80	4.15	22.750	0.289
C6	23.90	4.26	8.667	0.289
C7	30.40	4.49	10.000	0.115
C8	34.70	4.80	7.667	0.577

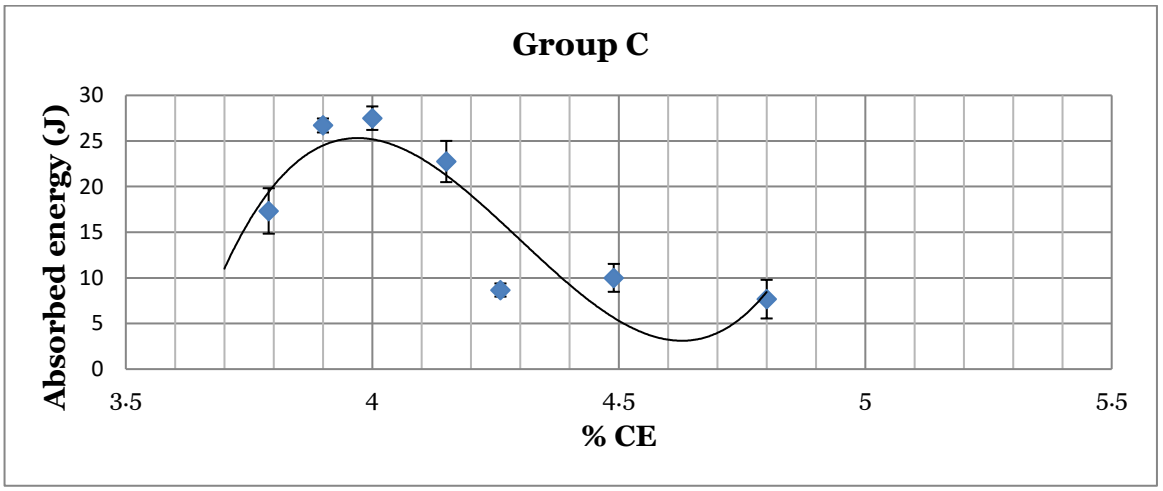

Figure 7. The effect of changing the % CE from 3.70 to 4.80 on absorbed energy of all heats for group C, varied nickel percent (Ni %) from 4.99 to 34.70

Data represented in Figures 5-7 give a spot of light on the absorbed energy of ductile austenitic cast iron near to the eutectic composition. Using carbon as alloying element to vary the % CE (Figure 5) did not affect the absorbed energy and give stable results around 21 J which afford the possibility to use this alloy with less attention to the variation of carbon percent subsequentially the % CE to produce reference specimens for low range in-direct calibrations of Charpy impact test machines since the measurements give a good precision with a standard deviation around 2 J, which is considered the subject of another work to discuss all requirements of the ISO 17034 including stability and homogeneity tests to produce reference material. Variation of silicon percent to control the % CE (Figure 6) lead to firstly almost stable region around 26 J at % CE from 3.86 to 4.28 and then decreasing behaviour to reach 12.7 J at 4.64 % CE. Finally, variation of nickel percent gives much influence on the absorbed energy as it show unstable region up to 3.79 % CE (Figure 7) which may be due to presence pearlitic-martensitic phases and rarity of nickel percent, and then splits the absorbed energy into two level; the first is about 23 J at % CE from 3.90 to 4.15 and the second level is about 8.5 J at % CE from 4.26 to 4.8, which may be relevant to the presence percent between the iron carbides as hard phase and the austenite as soft phase in the matrix. Generally, using carbon or silicon or as alloying elements to control the variation of % CE give absorbed energy values from 7 J to 27 J. These types of austenitic ductile cast iron could be used as an alternative to stainless steel to build the standard weights used in force, mass, and torque standard calibration machines.

IV. CONCLUSION

1. There is no measurable influence of % CE on the absorbed energy of group A, varied carbon percent (C %) ranging from 2.11 to 3.42, and the absorbed energy is about 21 J. While the absorbed energy decreased with increase the % CE for groups B and C, varied silicon percent (Si %) from 1.63 to 5.31, varied nickel percent (Ni %) from 4.99 to 34.70, respectively. The absorbed energy for group B is ranging from 12.7 J to 27 J and for group C it is ranging from 7.7 J to 27.5 J.
2. The variation of absorbed energy versus % CE showed the highest value of 22.197 J at % CE of 3.91 for group A. For group B, the highest value of absorbed energy was 27 J at % CE of 4.16. On the other hand, the highest value was 27.5 J at % CE of 3.9 for group C.
3. The measurements showed good repeatability as low standard deviations for the 3 groups A, B, and especially C. This observation leads to the possibility of producing a certified reference impact test material used for either in-direct verification or intermediate check of impact testing machines. The production of reference material is the subject of another work to discuss all requirements of the ISO 17034 including stability and homogeneity tests.

V. REFERENCES

AFS 2010, Ductile Iron Handbook Paperback-2010.

Ahmad, KM et al. 2016, 'Microstructure and mechanical properties of austentic ductile compacted cast iron with additive manganese', METAC Web of Conferences 74, 00009, ICMER.

Alzafin, YA et al. 2009, 'A study on the failure of pump castings made of ductile Ni-resist cast irons used in desalinations plants', Journal of Engineering Failure Analysis, vol. 14, no. 7, pp. 1294-1300.

Angus, HT 1978, Cast Iron: Physical and Engineering Properties, 2nd edn, British Cast Iron Research Association, London.

ASM International 1990, ASM Handbook, Volume 1: Properties and Selection: Irons, Steel, and high-performance alloys, vol. 1.

ASM International 2004, ASM Handbook, Volume 9: Metallography and Microstructures, vol. 9.

ASTM A439 / A439M – 18, Standard Specification for Austenitic Ductile Iron Castings.

Bai, J et al. 2022, 'Microstructures and Mechanical Properties of Ductile Cast Iron with Different Crystallizer Inner Diameters', Crystals, vol. 12(413). doi:

10.3390/cryst12030413.

Bayati, H & Elliott, R 1995, 'Relationship Between Structure and Mechanical Properties in High Mg Alloyed Ductile Iron', Materials Science and Technology, vol. 11, no. 3, pp. 284-293.

Fatahalla, Nabil et al. 1998, 'Microstructure and Mechanical Properties of SG-Iron in the CE Range from 3.78 to 5.24%', Zeitschrift für. Metallkunde, vol. 89, pp 507-513.

Fatahalla, Nabil et al. 2009, 'C, Si and Ni as alloying elements to vary carbon equivalent of austentic ductile cast iron: Micristructure and mechanical properties', Materials Science and Engineering: A, vol. 504, no. 1-2, pp. 81-89.

Hua, Qin et al. 2005, 'On-line prediction of carbon equivalent on high-nickel austenitic ductile iron', Materials Science and Engineering: A, vol. 393, no. 1-2, pp. 310-314.

ISO 148-1:2016, Metallic materials – Charpy pendulum impact test - Part 1: Test method.

Karaman, I et al. 2001, 'Competing Mechanisms and Modeling of Deformation in Austenitic Stainless Steel Single Crystals with and without Nitrogen', Acta Materialia, vol. 49, no. 19, pp. 3919-3933.

Karsay, SI 1987, 'Ductile Iron production Practice', Amer Foundry Society.

Moumeni, Elham 2013, 'Solidification of cast iron – A study on the effect of microalloy elements o cast iron', PhD thesis, Technical.

Nickel institute, Properties and application of Ni-resist and ductile Ni-resist alloys', viewed 19 August 2019, <https://www.nickelinstitute.org/media/1770/propertiesandapplicationsofni_resistandductileni_resistalloys_11018_.pdf>.

Shama, Shaik 2017, 'Comparison of Mechanical Properties of Ductile austenitic cast iron with Ferritic/Pearlitic Ductile Cast Iron', Master thesis, National Institute of Technology Rourkela Odisha, India.

University of Denmark, Downloaded from orbit.dtu.dk, viewed 20 June 2022, <https://backend.orbit.dtu.dk/ws/portalfiles/portal/77801669/Elham_Moumeni_Thesis..PDF>.

Zeng, DW et al. 2002, 'Investigation of laser surface alloying of copper on high Ni austenitic ductile iron', Materials Science and Engineering: A, vol. 333, no. 1-2, pp. 223-231.

Zhou, W et al. 2021, 'A steel-like unalloyed multiphase ductile iron', Journal of Materials Research and Technology, vol. 15, pp. 3836-3849.